Supporting Information

The Role of Terminal Functional Groups on Molecular Passivation of the Perovskite/Hole-Selective Layer Interface

Mahboubeh Hadadian,[a] Thomas W. Gries,[b] G. Krishnamurthy Grandhi,[c] Emil Rosqvist,[d] Rustem Nizamov,[a] Sari Granroth,[e] Paola Vivo,[c] Ronald Österbacka,[f] Jan-Henrik Smått,[d] Antonio Abate,[b] Kati Miettunen[a]*

[a] Department of Mechanical and Materials Engineering, Faculty of Technology, University of Turku, Vesilinnantie 5, Turku 20500, Finland, E-mail:mahboubeh.hadadian@utu.fi

[b] Helmholtz-Zentrum Berlin für Materialien und Energie (HZB), 14109, Berlin, Germany

[c] Hybrid Solar Cells, Faculty of Engineering and Natural Sciences, Tampere University, P.O. Box 541, Tampere FI-33720, Finland

[d] Laboratory of Molecular Science and Engineering, Henriksgatan 2, Åbo Akademi, Turku 20500, Finland

[e] Department of Physics and Astronomy, University of Turku, Turku 20014, Finland

[f] Physics and Center for Functional Materials, Faculty of Science and Engineering, Åbo Akademi University, Henriksgatan 2, Turku 20500, Finland

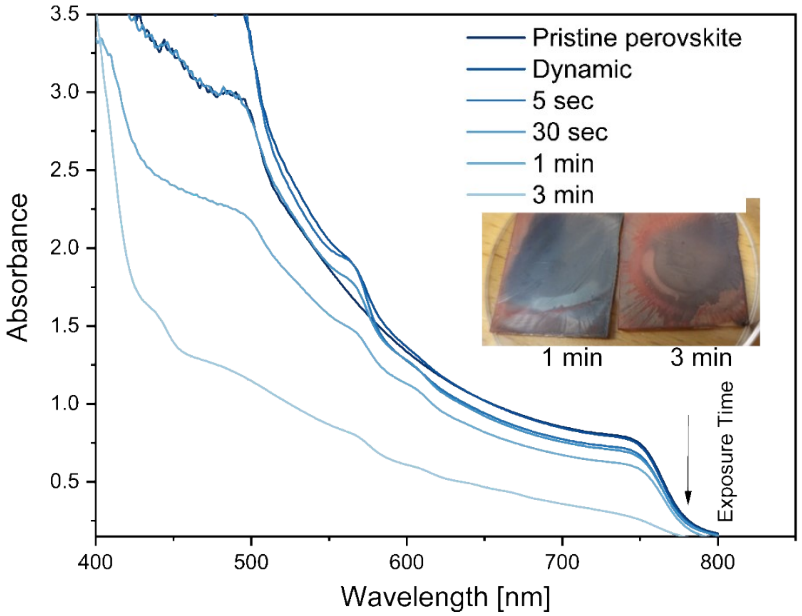

Figure S1. UV-vis absorption spectra of perovskite films with static deposition of the passivation layer in different time exposure before starting the spin coating. Dynamic means the deposition was done during the spin coating.

Figure S1 shows the decrease in the absorption of the sample by the time that the perovskite films was in contact with the solution of bulky organic cation in isopropanol (IPA) before starting the spin coating. Therefore, the samples were prepared using a mixture of solvents. Moreover, to avoid any damage to the perovskite layer even with the mixture of the solvents, the deposition was done dynamically.

Table S1. The fitted results of the $Pb^0/(Pb^0 + Pb^{2+})$ ratio for the perovskite film, after vacuum, first measurement, and sputtering time.

Condition	**Pristine**	**n-PentI**	**VA**	**5-AVAI**
first measurement	0.05	0.06	0.02	0.02
after some hours in vacuum	0.05	0.06	0.06	0.03
Depth profile, etched 20 s	0.08	0.19	0.08	0.06
Depth profile, etched 80 s	0.14	0.28	0.17	0.13

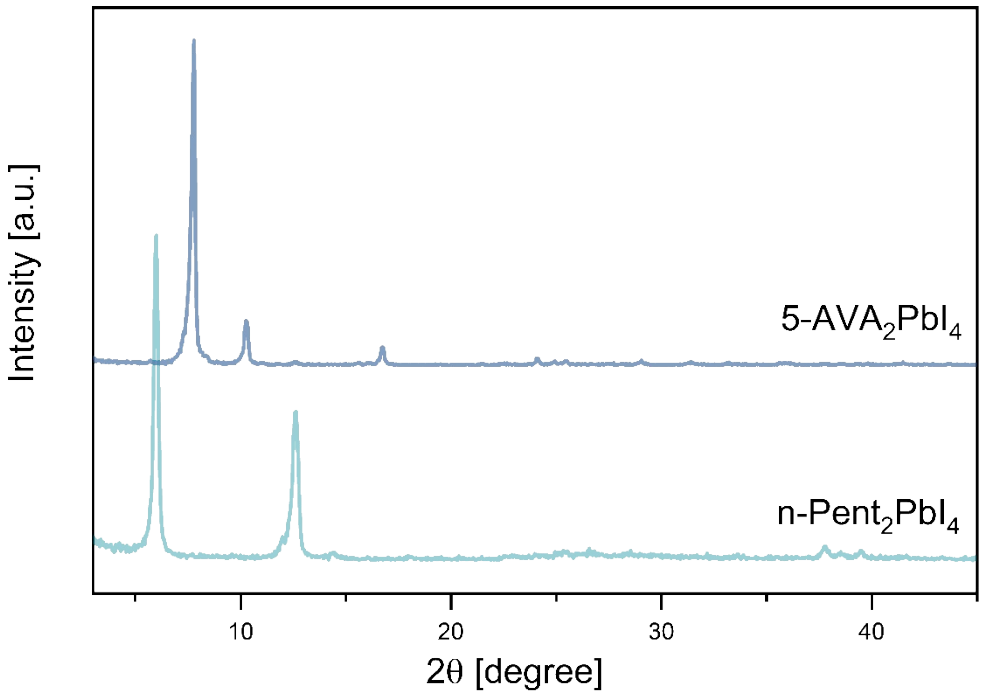

Figure S2. XRD pattern of pure 2D perovskites.

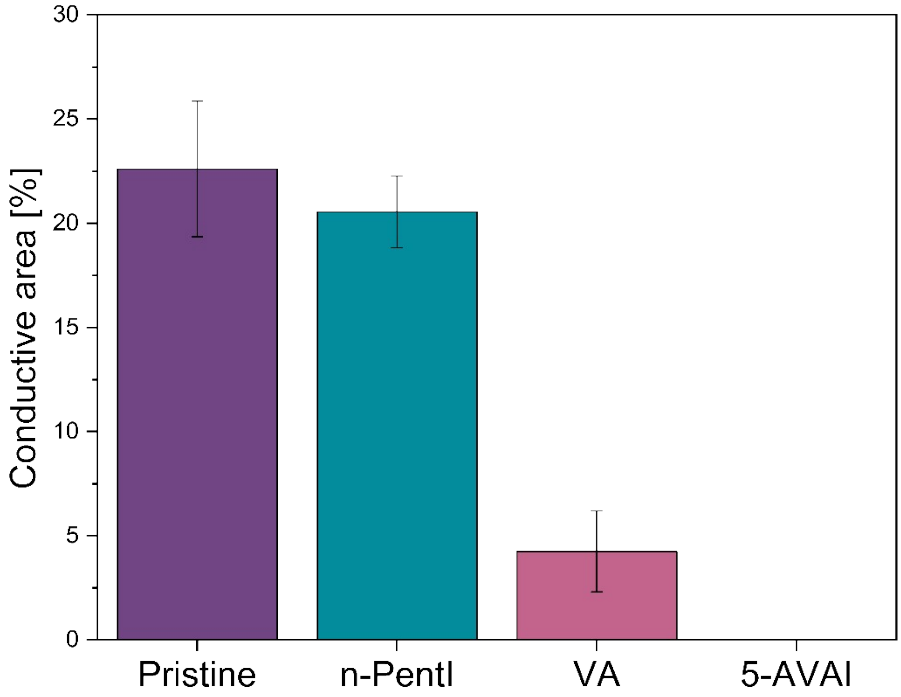

Figure S3. Relative conductive area (>40 pA) at 0.1V bias determined from C-AFM images. Error shown is the standard deviation (n=3).

Table. S2. Roughness parameter values of the different surfaces, with standard deviation (Std Dev) (n=4). Determined from 5 µm x 5 µm images with 512 pixel x 512 pixel resolution.

Parameter [unit]	Pristine	Std Dev	n-PentI	Std Dev	VA	Std Dev	5-AVAI	Std Dev
S_a [nm]	16.8	0.18	19.9	0.16	20.0	1.64	18.0	1.64
S_q [nm]	21.0	0.32	25.2	0.50	24.5	2.03	22.4	1.81
S_{sk} [-]	-0.12	0.029	-0.12	0.175	-0.01	0.094	0.02	0.047
S_{ku} [-]	2.95	0.23	3.30	0.53	2.91	0.12	2.92	0.29
S_{al} [µm]	0.35	0.016	0.37	0.009	0.38	0.026	0.41	0.021
S_{dr} [%]	4.40	0.68	3.96	0.08	5.67	0.39	2.20	0.17
S_{pd} [1/µm²]	8.31	0.50	5.45	1.50	5.68	1.16	3.61	0.48

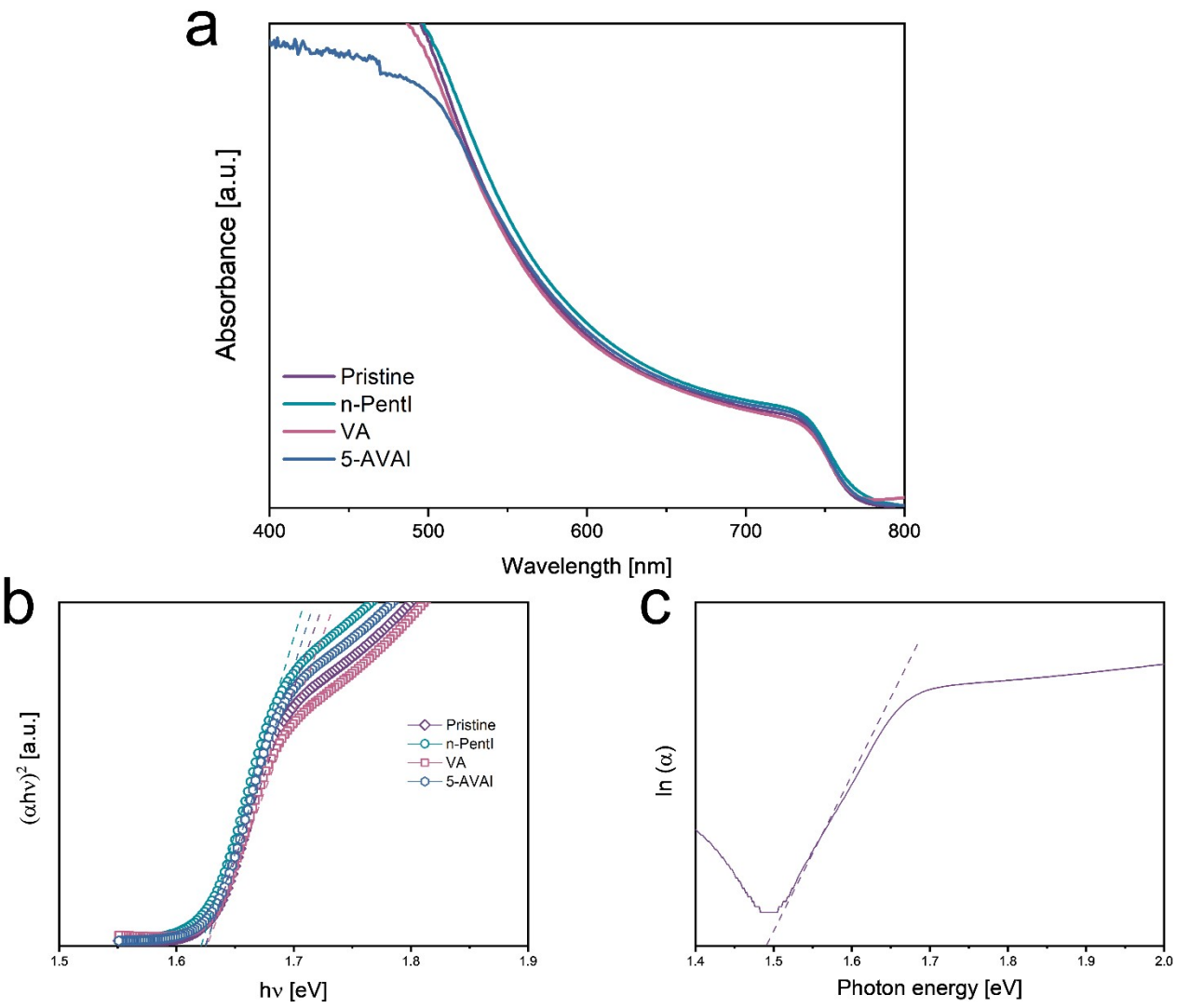

Figure S4. a. UV–vis absorption spectra, b. Tauc plot of the prepared treated and untreated perovskite films. c. Urbach energy (Eu) extracted from the absorption spectra by plotting the logarithm of absorption coefficient versus photon energy.

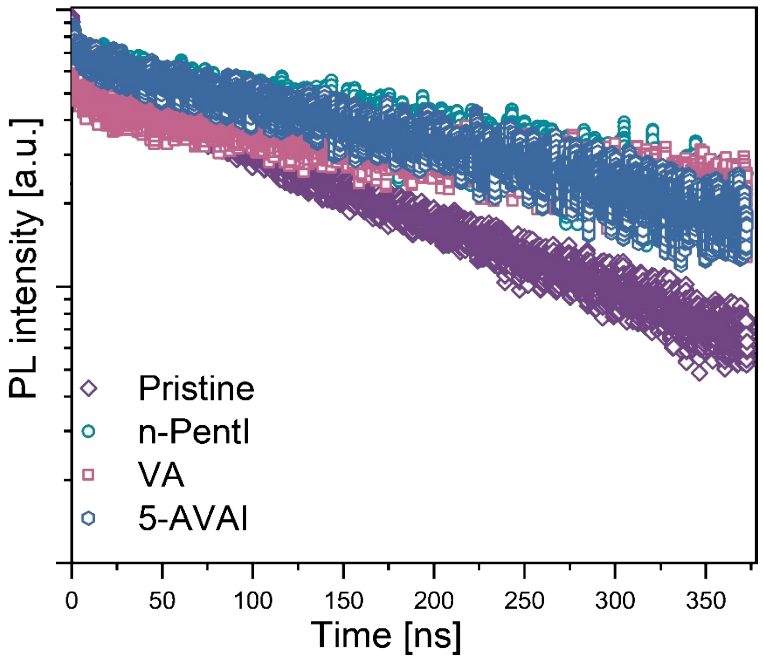

Figure S5. TRPL of the perovskite films.

Supporting Note 1

The differential lifetime (τ_{PL}) can be calculated as:

$$\tau_{PL} = \left(\frac{-1}{m}\frac{-dln(\Phi_{PL})}{dt}\right)^{-1}$$

where Φ_{PL} is the TRPL intensity at time t, and m is the injection level in the perovskite layer, which we consider to be 2 for perovskite, an intrinsic semiconductor. In line with the observed PL intensity quenching trends for the pristine and passivated samples in the presence of spiro-OMeTAD HSL, their PL lifetime decay values are accelerated at high PL intensities (i.e., short delay times) in the presence of spiro-OMeTAD HSL, except for 5-AVAI/HSL, indicating the transfer of photogenerated holes from the perovskite into the HSL. Furthermore, the plots of ln(Φ_{PL}), a relative measure of the quasi-Fermi level splitting, versus lifetime show that the constant part is typically attributed to the recombination (Shockley-Read-Hall (SRH)-type) of the photogenerated carriers via traps. The point at which the lifetime trend saturates can be considered as the bulk SRH lifetime. A bulk SRH lifetime of 370 ns for the pristine perovskite sample is comparable to previously reported values.[1] Similarly, the effective SRH lifetime for the HSL-containing samples, which involves a complex interplay of

bulk SRH recombination, surface recombination velocity (S), and the energy offset at the interface between the two layers, is reduced. We extracted the value of S using the following expression:

$$\tau_{eff.\ SRH} = \left(\frac{1}{\tau_{bulk\ SRH}} + \frac{S}{2d}\right)^{-1}$$

S value of 1245 cm/s is obtained for a perovskite layer thickness (d) of 500 nm in the perovskite/spiro-OMeTAD sample. The S values remain comparable, ranging from 945 to 1245 cm/s, for the perovskite/HSL samples with n-Pentl and VA and without any interlayer, consistent with their comparable hole injection yields shown in Figure 3b**.** Thus, n-Pentl effectively passivates the surface traps of the perovskite layer while allowing efficient hole transfer into the HSL.

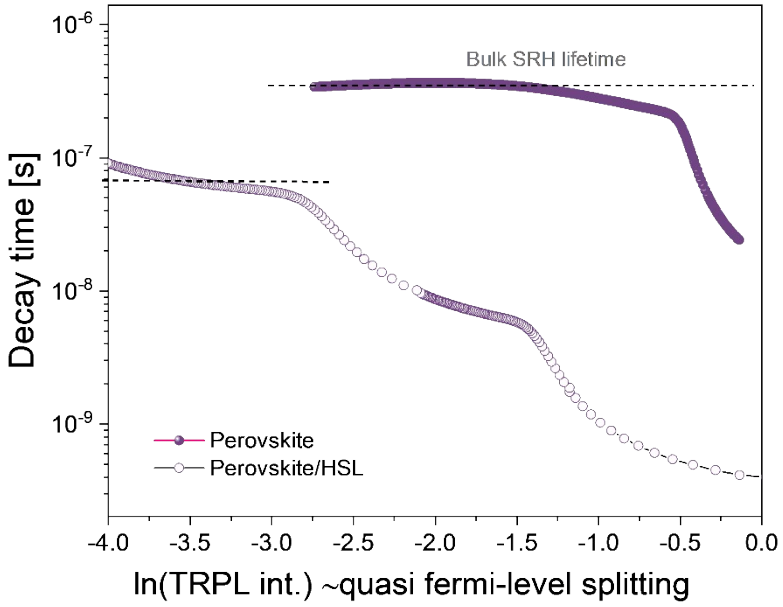

Figure S6. Differential lifetime as a function of the logarithm of TRPL intensity for perovskite and peroskite/HSL samples.

Figure S7a presents a color map of the trSPV signals as a function of logarithmic time and photon energy, providing insights into charge separation processes across a broad range of excitation wavelengths.[2] As the figure shows, all perovskite films incorporating spiro-OMeTAD exhibit a distinct SPV response, indicative of efficient photogenerated charge separation at the perovskite/HSL interface. A small degree of sub-bandgap (<1.6 eV) charge separation is observed, suggesting the presence of tail states that influence to charge carrier dynamics.[3] The characteristic time (t_{max}), at which the SPV signal reaches its peak, varies across the samples, reflecting differences in interfacial charge behavior. The untreated perovskite interface exhibits the shortest t_{max}, indicating rapid charge separation. In contrast, the 5-AVAI-treated interface displays the longest t_{max}, implying prolonged charge retention and reduced recombination losses.

Figure S7b displays trSPV measurements performed on pristine and treated perovskite layers at two photon wavelengths: 563 nm (2.2 eV), and 476 nm (2.6 eV). Higher photon energies generate charge carriers closer to the HSL. The trSPV signal is directly proportional to the separated charges at the interface.[4] The n-PentI-treated perovskite film exhibits the highest SPV signal across all excitation wavelengths, suggesting superior charge separation efficiency and reduced recombination losses, likely due to more effective surface passivation and optimized energy band alignment at the interface. In contrast, the pristine sample shows the weakest SPV response, likely attributable to a higher density of surface trap states and non-radiative recombination pathways.

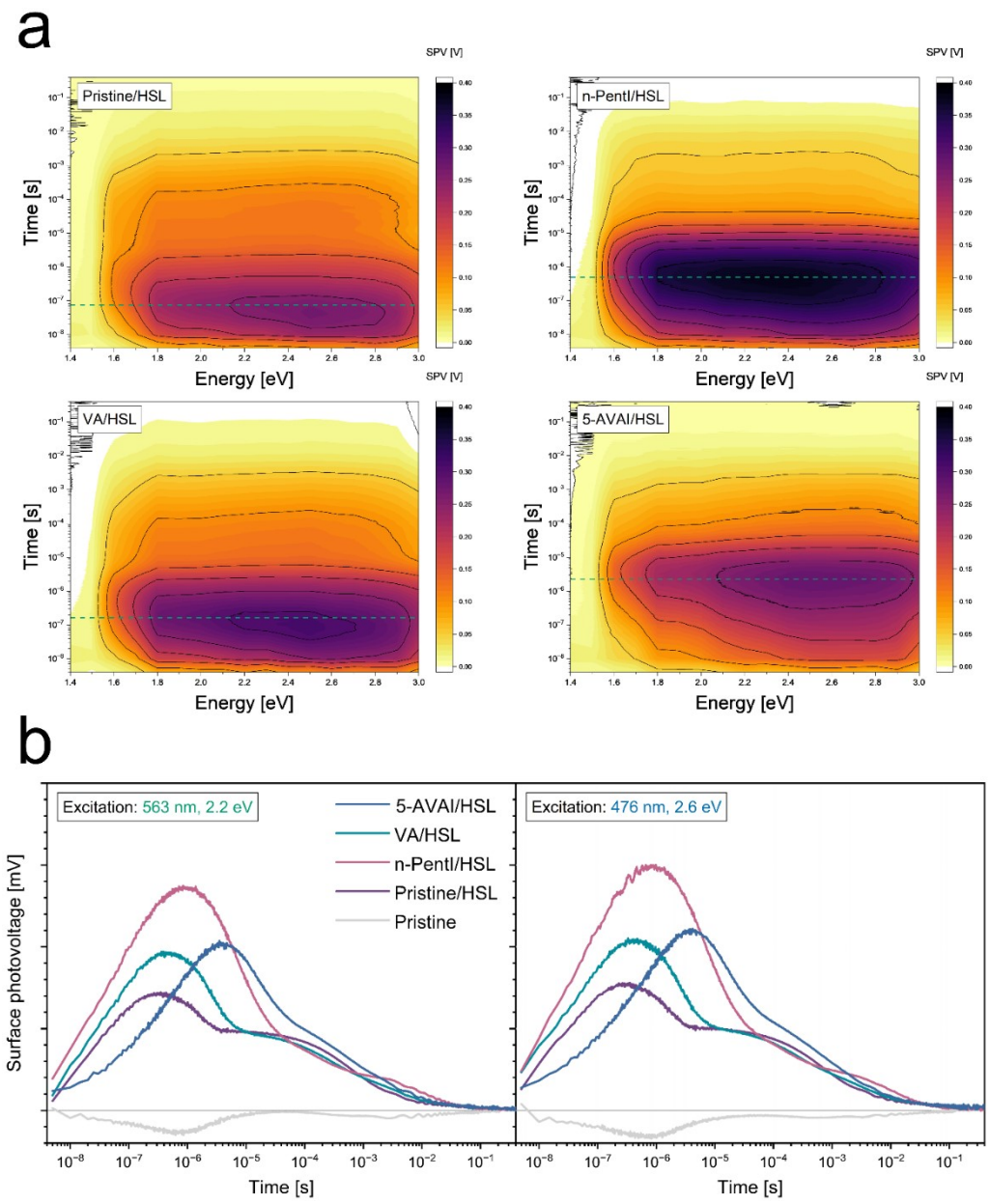

Figure S7. a. Contour plots of pristine perovskite, n-PentI treated perovskite, VA treated perovskite, and 5-AVAI treated perovskite with spiro-OMeTAD. b. Transient SPV of perovskite films measured at excitation sources of 563 nm (left), and 476 nm (right).

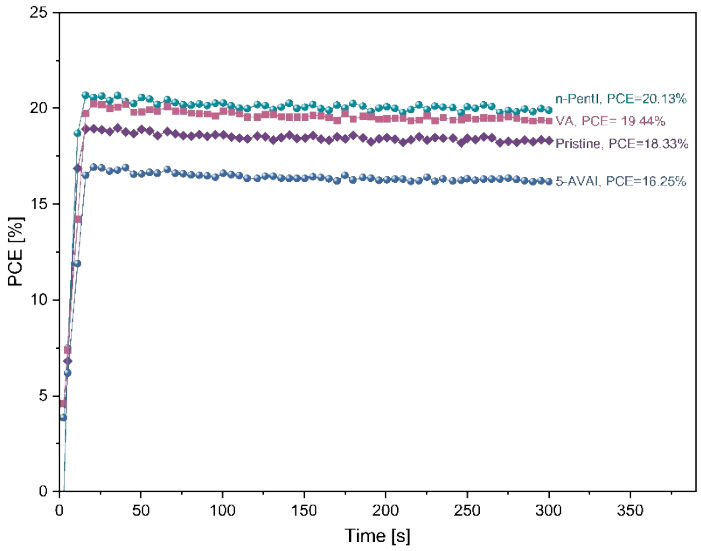

Figure S8. Stabilized PCEs of the champion pristine and PSCs based on surface modified perovskite absorber layers measured under continuous 1-Sun illumination at ambient conditions.

Table S3. Average photovoltaic performance parameters (reverse scan direction) with standard deviations.

Perovskites	V_{OC} **[V]**	J_{SC} **[mAcm^{-2}]**	***FF***	***PCE* [%]**
Pristine	1.07±0.04	22.3±1.1	0.69±0.05	16.32±1.8
n-PentI	1.10±0.02	22.5±0.9	0.73±0.03	18.03±1.2
VA	1.09±0.02	22.5±1.3	0.74±0.03	18.12±1.3
5-AVAI	1.08±0.03	22.0±1.1	0.64±0.06	15.72±1.9

To confirm the meaningful changes, we have expanded our statistical analysis on V_{OC} values (Figure S9), showing the Analysis of Variance (ANOVA). We show that the V_{OC} differences from pristine perovskite to n-PentI and VA perovskite-based devices are small but statistically significant ($p < 0.05$). The figure show Tukey test, the after ANOVA found the difference, showing the meaningful difference for n-PentI and VA surface treated samples in comparison to the pristine perovskite.

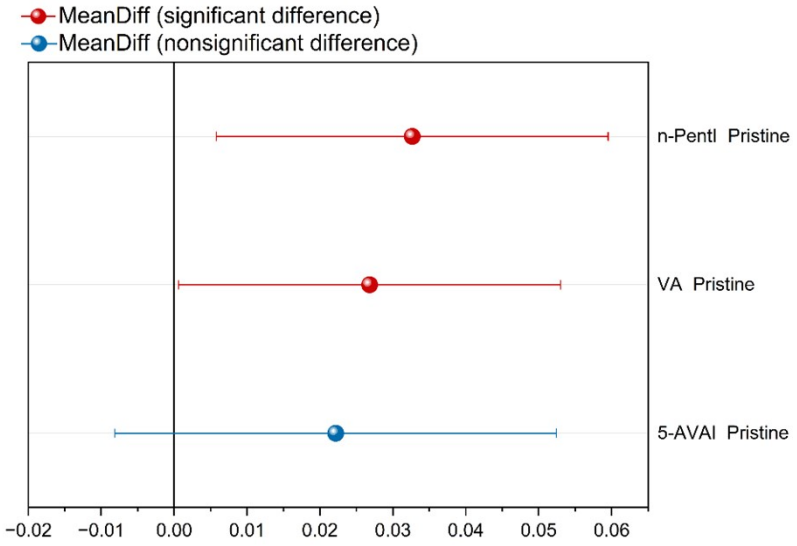

Figure S9. Tukey's HSD post hoc comparison of mean values among Pristine, n-PentI, VA, and 5-AVAI groups. Error bars indicate 95% confidence intervals; groups not sharing a letter differ significantly at $p < 0.05$.

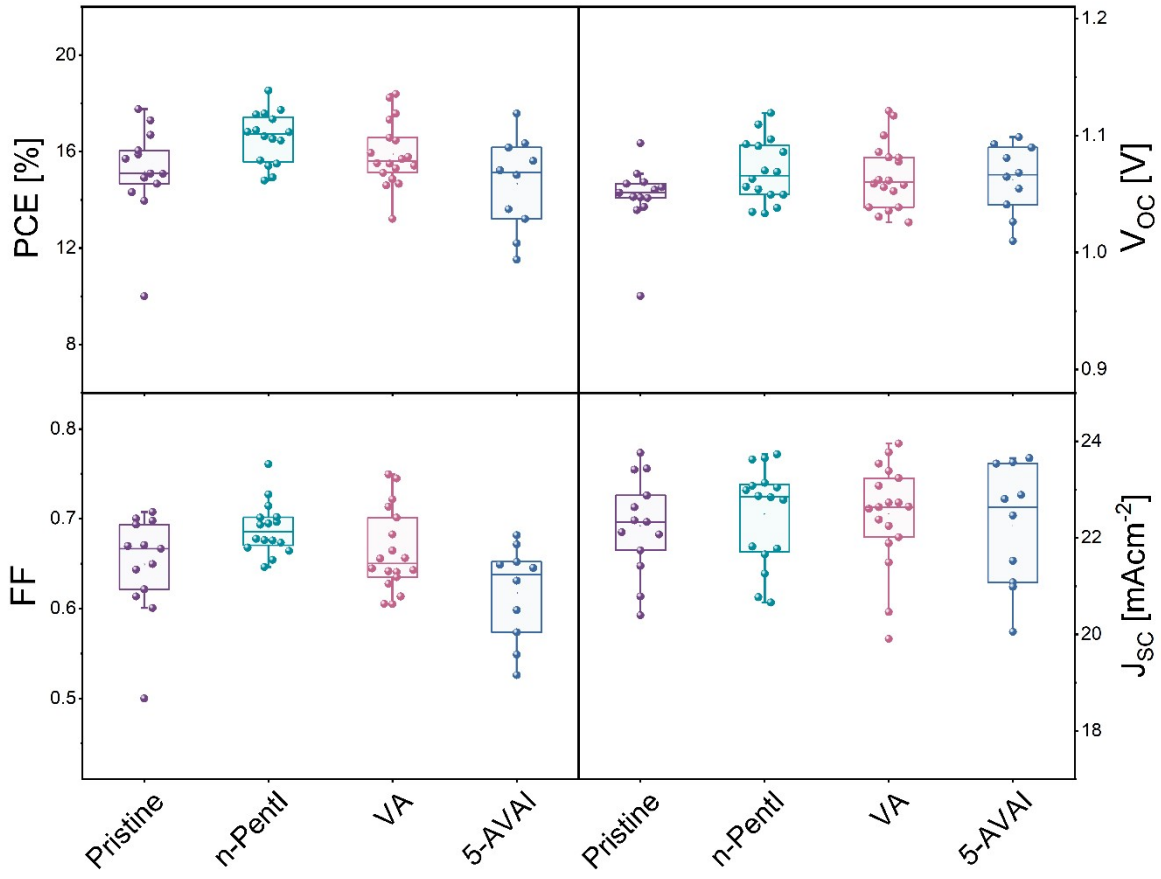

Figure S10. Statistical distribution of photovoltaic parameters from the forward scan direction.

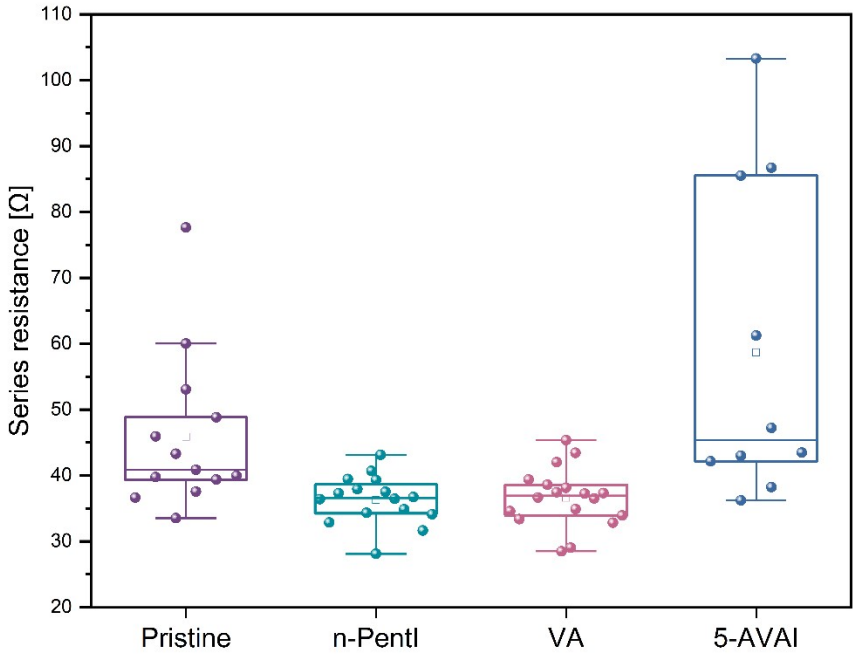

Figure S11. Statistical distributions of series resistance values of devices.

References

1 M. Liu, S. Dahlström, C. Ahläng, S. Wilken, A. Degterev, A. Matuhina, M. Hadadian, M. Markkanen, K. Aitola, A. Kamppinen, J. Deska, O. Mangs, M. Nyman, P. D. Lund, J.-H. Smått, R. Österbacka and P. Vivo, *J. Mater. Chem. A*, 2022, **10**, 11721–11731.
2 Z. Iqbal, T. W. Gries, A. Musiienko and A. Abate, *Solar RRL*, 2024, **8**, 2400329.
3 B. Wang, W. Chu, Y. Wu, W. A. Saidi and O. V. Prezhdo, *npj Comput Mater*, 2025, **11**, 1–9.
4 Z. Iqbal, T. W. Gries, A. Musiienko and A. Abate, *Solar RRL*, 2024, **8**, 2400329.